Supplementary Material

1 DISCRETIZATION ERROR COMPARISON OF DISPERSION-REDUCED FEMS AND STANDARD FEMS

This section briefly explains the accuracy of the dispersion-reduced FEMs in time and frequency domains against standard FEMs using conventional Hex8 from the theoretical aspects. Here, the discretization error characteristics in both dispersion-reduced and standard FEMs are compared in the case of sound propagation in a free field. We consider a plane wave propagation in a free field that is discretized by Hex8, as shown in Figure S1. In the figure, the element size of Hex8 in each direction is denoted by d_x, d_y and d_z, respectively. Also, θ and ϕ represent the elevation and azimuth in a spherical coordinate system. Detailed procedure of this discretization error analysis can be found in the literature (Okuzono et al., 2012).

In the time domain, the discretization error is generally defined as the relative error between an exact sound speed c and a numerical sound speed $\tilde{c}$. For standard TD-FEM using conventional Hex8 for spatial discretization and Fox–Goodwin method for time integration, the discretization error is given as (Okuzono et al., 2012)

$$\frac{|c-\tilde{c}|}{c} \simeq \frac{k^2}{24}[d_x^2\cos^4\phi\sin^4\theta + d_y^2\sin^4\phi\sin^4\theta + d_z^2\cos^4\theta] + \mathcal{O}[k^4 d_{x,y,z}^4 + (c\Delta t)^4], \tag{S1}$$

where k is the wavenumber, and Δt is the time interval. The Eq. (S1) expresses that the standard TD-FEM has second-order accuracy regarding the discretization error. Notably, the standard TD-FEM does not have a second-order error term with respect to time. Therefore, the standard TD-FEM has fourth-order accuracy in time by using Fox–Goodwin method. This is the reason for using Fox–Goodwin method. On the other hand, the dispersion-reduced TD-FEM can eliminate the second-order error term in Eq. (S1) and it has the fourth-order accuracy in terms of the discretization error, which is expressed as (Okuzono et al., 2012)

$$\frac{|c-\tilde{c}|}{c} \simeq \frac{k^4}{480}[d_x^4\cos^6\phi\sin^6\theta + d_y^4\sin^6\phi\sin^6\theta + d_z^4\cos^6\theta - c^4\Delta t^4] + \mathcal{O}[k^6 d_{x,y,z}^6 + (c\Delta t)^6], \tag{S2}$$

To show the accuracy of the dispersion-reduced TD-FEM, Figure S2**(A)**,**(B)** respectively presents discretization errors of the dispersion-reduced TD-FEM and the standard TD-FEM in all sound wave propagation directions (θ, ϕ). In those calculations, we considered that $k = 4\pi$ and 8π with the element size of $d_x = d_y = d_z = 0.05\,\mathrm{m}$. The time interval was set to the stability limit value. Note that the case of $k = 4\pi$ corresponds to the discretization that follows the well-known rule of thumb for the linear elements, i.e., ten elements per wavelength. The case of $k = 8\pi$ corresponds to the discretization at five elements per wavelength. For the case of $k = 4\pi$, the dispersion-reduced TD-FEM shows significantly higher accuracy than the standard TD-FEM. The maximum relative error of the dispersion-reduced TD-FEM is less than 0.029% whereas that of the standard TD-FEM shows 1.6% relative error. Furthermore, the dispersion-reduced TD-FEM shows significantly lower discretization error with the maximum relative error less than 0.46%, even in the use of coarser mesh case of $k = 8\pi$. A recent solution convergence study (Okuzono et al., 2019) using an impedance tube problem also revealed that the dispersion-reduced

TD-FEM that uses a mesh of spatial resolution of five elements per wavelength shows higher accuracy than the standard TD-FEM that uses a mesh discretized by the rule of thumb of ten elements per wavelength.

In the frequency domain, the discretization error is generally defined as the relative error between an exact wavenumber k and a numerical wavenumber $\tilde{k}$. Unlike a time domain analysis, only spatial discretization error is introduced. For standard FD-FEM using conventional Hex8, the dispersion error is given as (Okuzono and Sakagami, 2018).

$$\frac{|k-\tilde{k}|}{k} \simeq \frac{k^2}{24}[d_x^2 \cos^4\phi \sin^4\theta + d_y^2 \sin^4\phi \sin^4\theta + d_z^2 \cos^4\theta] + \mathcal{O}[k^4 d_{x,y,z}^4]. \tag{S3}$$

The above equation shows that the standard FD-FEM has second-order accuracy and the function form of the error has the same as that in Eq. (S1) of the standard TD-FEM. That means that the TD-FEM and FD-FEM include the same magnitude of spatial discretization error when using the same finite elements for spatial discretization. This is also true for the dispersion-reduced FEMs. For the dispersion-reduced FD-FEM, the discretization error is defined as (Okuzono and Sakagami, 2018)

$$\frac{|k-\tilde{k}|}{k} \simeq \frac{k^4}{480}[d_x^4 \cos^6\phi \sin^6\theta + d_y^4 \sin^6\phi \sin^6\theta + d_z^4 \cos^6\theta] + \mathcal{O}[k^6 d_{x,y,z}^6] \tag{S4}$$

The above equation has the same spatial discretization error term as that in Eq. (S2), and does not include the time discretization error term $-\frac{k^4}{480}c^4\Delta t^4$, which is included in Eq. (S2) for the dispersion-reduced TD-FEM. Since the contribution of the time discretization error term in Eq. (S2) is trivial, the dispersion-reduced TD-FEM and FD-FEM have almost the same discretization error characteristics. For the cases at $k = 4\pi$ and 8π using the element size of $d_x = d_y = d_z = 0.05\,\mathrm{m}$, the dispersion-reduced FD-FEM shows the maximum discretization errors of 0.033% and 0.46%, respectively. Meanwhile, when using different time intervals $\Delta t = \Delta t_{\mathrm{limit}}$, $0.5\Delta t_{\mathrm{limit}}$ and $0.25\Delta t_{\mathrm{limit}}$ where $\Delta t_{\mathrm{limit}}$ represents the time interval at the stability limit, the dispersion-reduced TD-FEM shows the maximum errors of 0.029%, 0.033% and 0.033% for $k = 4\pi$ respectively. For $k = 8\pi$, their maximum errors show 0.46%, 0.52% and 0.52%, respectively. Note that a recent study (Okuzono and Sakagami, 2018) also showed that the dispersion-reduced FD-FEM that uses a mesh of spatial resolution of five elements per wavelength provides higher accurate solution than the standard FD-FEM using a mesh discretized by the rule of thumb of ten elements per wavelength.

2 INITIAL VALUE SELECTION EFFECT ON CONVERGENCE OF ITERATIVE SOLVERS

This section briefly presents preliminary experimental results of how initial values selection of iterative solvers affects its convergence in TD-FEM and FD-FEM. As described in Sections 2.1 and 2.2, the CG and CSQMOR methods were used respectively for TD-FEM and FD-FEM with a diagonal scaling preconditioning. We examined convergence speed using two initial value setups via the small cubic room problem and the meeting room problem used in Section 3. Here, only the results for the meeting room problem are presented since the small cubic problem results showed the same conclusion. The first setup uses zeros to the initial value $\boldsymbol{x}_0$ of the iterative solver. We denote this setup as $\boldsymbol{x}_0 = \boldsymbol{0}$. Another setup uses solutions in the previous time step or frequency as $\boldsymbol{x}_0$, denoted by $\boldsymbol{x}_0 = \boldsymbol{x}^{n-1}$.

As the results, Figure S3**(A)**,**(B)** respectively present a comparison of iteration numbers between two initial value setups $\boldsymbol{x}_0 = \boldsymbol{0}$ and $\boldsymbol{x}_0 = x^{n-1}$ for TD-FEM and FD-FEM. For TD-FEM, results showed that CG method with the setup $\boldsymbol{x}_0 = \mathbf{0}$ converges with one less iteration number at almost all time steps compared with the setup of $\boldsymbol{x}_0 = \boldsymbol{x}^{n-1}$. Conversely, for FD-FEM, a marked performance was obtained by the setup of $\boldsymbol{x}_0 = \boldsymbol{x}^{n-1}$. As shown in Figure S3(**B**), CSQMOR method with the setup of $\boldsymbol{x}_0 = \boldsymbol{x}^{n-1}$ outperforms the setup of $\boldsymbol{x}_0 = \mathbf{0}$ with fewer iteration numbers at almost all frequencies. Quantitatively, the average reduction rate of iteration number using the setup $\boldsymbol{x}_0 = \boldsymbol{x}^{n-1}$ to the $\boldsymbol{x}_0 = \mathbf{0}$ reaches 22%. As an example to show the effectiveness of the setup $\boldsymbol{x}_0 = \boldsymbol{x}^{n-1}$, Figure S4 shows a comparison of convergence history at 1500 Hz between $\boldsymbol{x}_0 = \mathbf{0}$ and $\boldsymbol{x}_0 = \boldsymbol{x}^{n-1}$. Here, the relative residual 2-norm in the figure is defined as $||\boldsymbol{A}\boldsymbol{x}_i - \boldsymbol{b}||_2/||\boldsymbol{b}||_2$, where $\boldsymbol{A}$ and $\boldsymbol{b}$ are respectively the coefficient matrix and right-hand side vector of the linear system, and $\boldsymbol{x}_i$ is the approximate solution at i-th iteration. It is found that $\boldsymbol{x}_0 = \boldsymbol{x}^{n-1}$ can start the computation with one order smaller residual 2-norm value at the first iteration. At all iterations, $\boldsymbol{x}_0 = \boldsymbol{x}^{n-1}$ presents lower residual 2-norm than that of $\boldsymbol{x}_0 = \mathbf{0}$, and consequently it achieves faster convergence. From those results, we chose the setup $\boldsymbol{x}_0 = \mathbf{0}$ for TD-FEM and $\boldsymbol{x}_0 = \boldsymbol{x}^{n-1}$ for FD-FEM, respectively. Note that it can be an effective way to use a solution in the previous frequency results as an initial value of the iterative solver for FD-FEM when calculating room impulse responses. However, for its generalization, further investigations will be necessary from various aspects, e.g., the effect of frequency interval and the type of iterative solvers.

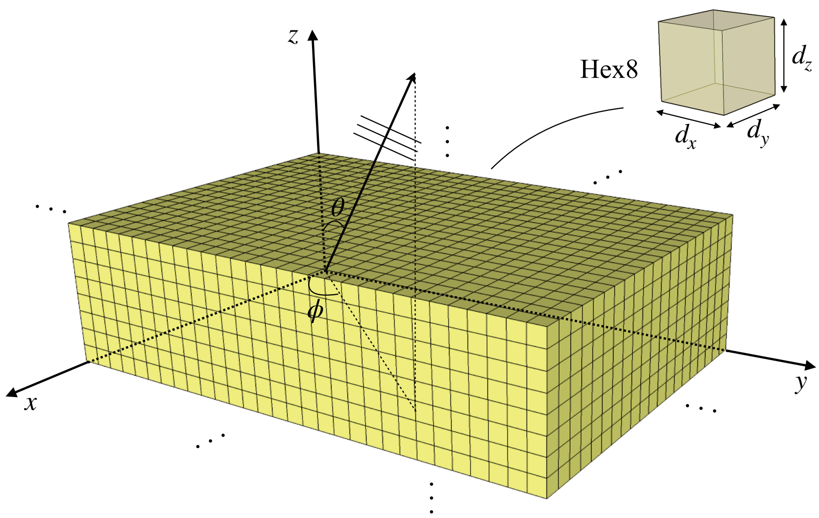

Figure S1. Plane wave propagation in a free field discretized using Hex8.

REFERENCES

Okuzono, T., Otsuru, T., Tomiku, R., and Okamoto, N. (2012). Application of modified integration rule to time-domain finite-element acoustic simulation of rooms. *The Journal of the Acoustical Society of America* 132, 804–813. doi:10.1121/1.4730920

Okuzono, T. and Sakagami, K. (2018). A frequency domain finite element solver for acoustic simulations of 3D rooms with microperforated panel absorbers. *Applied Acoustics* 129, 1–12. doi:10.1016/j.apacoust.2017.07.008

Okuzono, T., Shimizu, N., and Sakagami, K. (2019). Predicting absorption characteristics of single-leaf permeable membrane absorbers using finite element method in a time domain. *Applied Acoustics* 151, 172–182. doi:10.1016/j.apacoust.2019.03.006

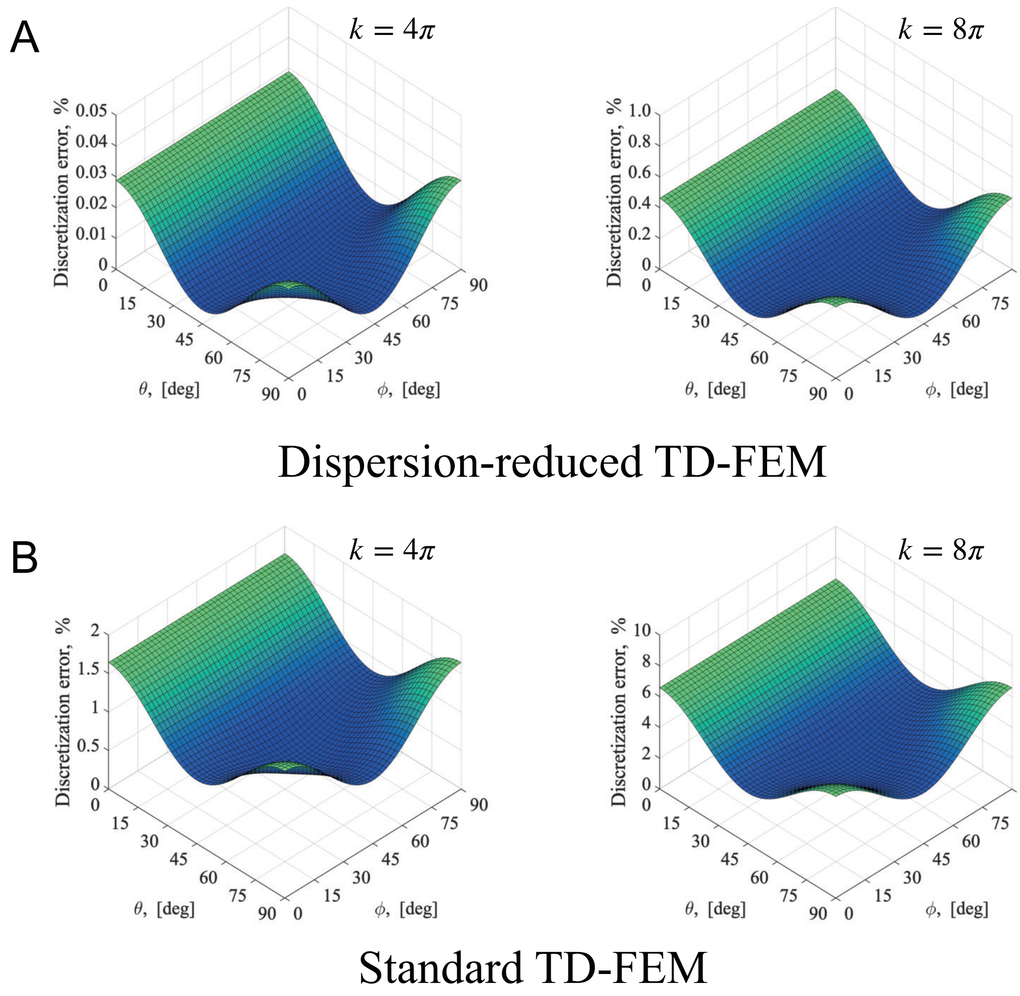

Figure S2. Discretization errors at $k = 4\pi$ (left) and at $k = 8\pi$ (right) for **(A)** the dispersion-reduced TD-FEM and **(B)** the standard TD-FEM.

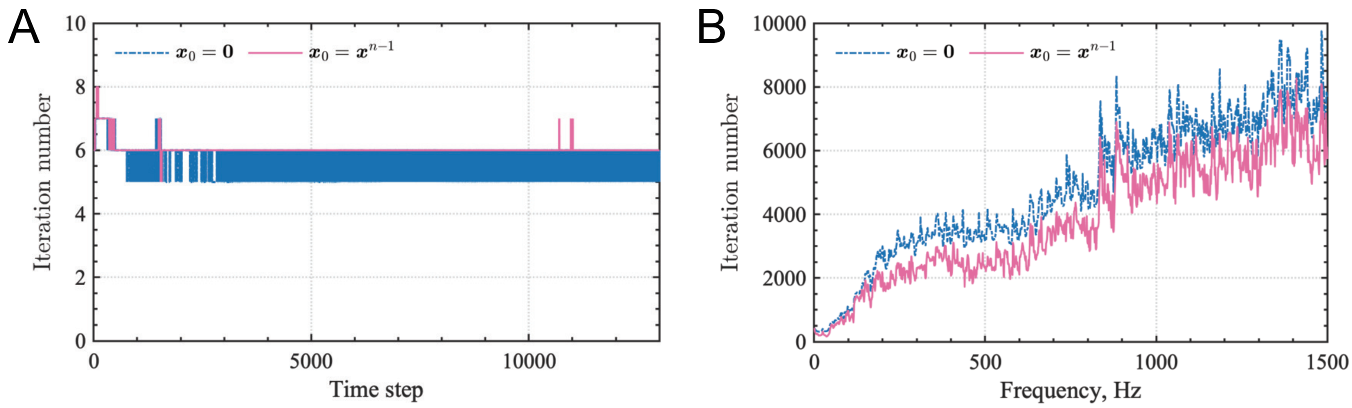

Figure S3. Comparison of iteration numbers between two initial value setups $\boldsymbol{x}_0 = \mathbf{0}$ and $\boldsymbol{x}_0 = \boldsymbol{x}^{n-1}$: **(A)** iteration numbers at each time step in TD-FEM and **(B)** iteration numbers at each frequency in FD-FEM. TD-FEM and FD-FEM, respectively, use CG method and CSQMOR method with diagonal scaling preconditioning.

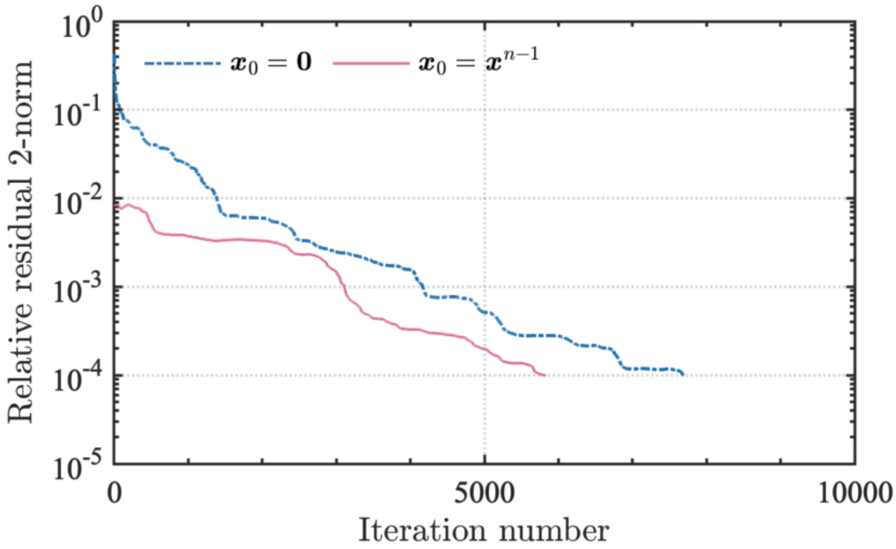

Figure S4. Comparison of convergence history of CSQMOR method at 1500 Hz between two initial value setups $\boldsymbol{x}_0 = \mathbf{0}$ and $\boldsymbol{x}_0 = \boldsymbol{x}^{n-1}$.